Sensitivity of the GFDL Modular Ocean Model to Parameterization of Double-Diffusive Processes*

JUBAO ZHANG

MIT/WHOI Joint Program, Department of Physical Oceanography, Woods Hole Oceanographic Institution, Woods Hole, Massachusetts

RAYMOND W. SCHMITT AND RUI XIN HUANG

Department of Physical Oceanography, Woods Hole Oceanographic Institution, Woods Hole, Massachusetts

(Manuscript received 24 February 1997, in final form 7 July 1997)

ABSTRACT

The effect of double-diffusive mixing on the general circulation is explored using the GFDL MOM2 model. The motivation for this comes from the known sensitivity of the thermohaline circulation to the vertical diffusivity and the earlier work of Gargett and Holloway, who studied the effects of a simple nonunity ratio between heat and salt diffusivities in a GCM. In this work, a more realistic, yet conservative, parameterization of the double-diffusive mixing is applied, with the intensity depending on the local density ratio $R_\rho = \alpha T_z/\beta S_z$. A background diffusivity is used to represent non-double-diffusive turbulent mixing in the stably stratified environment. The numerical model is forced by relaxation boundary conditions on both temperature and salinity at the sea surface. Three control experiments have been carried out: one with the double-diffusive parameterization (DDP) determined by the local density ratio, one with constant but different diffusivities for heat and salt as previously considered by Gargett and Holloway (GHD), and the other with the same constant diapycnal eddy diffusivity for both heat and salt (CDD). The meridional overturning in run DDP is 22% less than in run CDD, and the maximum poleward heat transport is about 8% less. In comparison, the overturning rate and poleward heat transport in run GHD display reductions that are about half as large. The interior temperature and salinity in run DDP and GHD are higher than in run CDD, with the change in run DDP more than twice that in run GHD. In addition, in DDP and GHD, the density ratio distribution becomes closer to unity than in run CDD, with the change in run DDP being larger than in GHD. Interestingly, the double diffusion is stronger in the western boundary current region than the interior, implying a close relation between vertical shear and the intensity of double diffusion. These results indicate a greater sensitivity of the thermohaline circulation to double diffusion than had previously been suspected due to the tendency of the double-diffusive mixing to generate self-reinforcing flows. This effect appears to be more significant when the double-diffusive mixing is applied only when the stratification is favorable rather than uniformly applied. In addition, parameter sensitivity experiments suggest that double diffusion could have stronger effects on the meridional overturning and poleward heat transport than modeled here since the parameterizations chosen are rather conservative.

1. Introduction

The thermohaline circulation of the ocean plays an important role in the climate system of the earth, especially in controlling the oceanic part of the poleward heat transport. The large-scale structure of the thermohaline circulation and its variability has been studied extensively in models (Weaver and Hughes 1992; Huang 1995). One result of these studies is the finding that the strength of the meridional overturning cell (MOC) is strongly dependent on the value of the vertical (or diapycnal) eddy diffusivity (K), which is the mechanism that provides the necessary warming of the rising abyssal waters. F. Bryan (1987) found an approximate $K^{1/3}$ dependence of the MOC; however, his model runs may not have reached equilibrium; later work has found a $K^{2/3}$ dependence (Marotzke 1997; Zhang et al. 1997, submitted to *J. Phys. Oceanogr.*), when the conventional ''relaxation'' boundary conditions are applied for the surface forcing. Whatever the specific power law dependence, the continual production of cold deep water at high latitudes requires vertical mixing to close the circulation (Munk 1966).

Observational microstructure work in recent years (Gregg 1989; Polzin et al. 1995) has indicated that turbulent mixing in the ocean interior caused by internal wave breaking is generally much weaker than has been inferred from the large-scale budget approach of Munk (1966), Hogg et al. (1982), and others. However, evi-

* WHOI Contribution Number 9239.

Corresponding author address: Mr. Jubao Zhang, Room 54-1419, Massachusetts Institute of Technology, Cambridge, MA 02139.
E-mail: jubao@mit.edu

dence is emerging that turbulence near rough topography may be sufficiently enhanced to provide the required downward heat flux (Toole et al. 1994; Polzin et al. 1997). One problem with near-bottom mixing is that the stratification is weak in the abyss, so heat fluxes tend to be small, even with very large eddy diffusivities. This reduced effectiveness of deep internal-wave-induced turbulence (the mixing of already mixed water) leads us to examine the other mixing processes occurring in the more strongly stratified thermocline.

The primary processes that must be considered are the double-diffusive instabilities of salt fingering, which occurs when temperature and salinity both decrease with depth, and diffusive convection, which occurs when temperature and salinity both increase with depth. It is well known that on the molecular level heat and salt have diffusivities that are two orders of magnitude different. This difference drives convective motions even if the overall density profile is stable. Substantial evidence is now available that these processes play a significant role in ocean mixing (Schmitt 1994). Their principal effect is to transport heat and salt at different rates in the vertical and cause a net upgradient flux of buoyancy. A number of recent modeling studies show that such differential transports have important effects on the stability and structure of the large-scale thermohaline circulation.

In particular, Gargett and Holloway (1992, hereafter GH92) first investigated the effects of a simple double-diffusive parameterization in an ocean model. They showed that the steady-state characteristics of low-resolution GCMs used in climate studies are very sensitive to the ratio of the vertical eddy diffusivities for salinity and temperature. Large differences in meridional transports resulted due to the upgradient buoyancy flux, which forced different advective–diffusive balances to be realized. Ruddick and Zhang (1989) found that the ''salt oscillator'' mechanism in a box model could be completely stabilized by incorporating salt fingers into the model. Most recently, Gargett and Ferron (1996) found that multibox models with nonequal heat and salt diffusivities exhibited extended ranges of multiple equilibria, a different mode transition near present-day values of freshwater forcing magnitude, and the possibility of quasiperiodic oscillatory states compared to an equal diffusivity run. Climate models generally neglect the double-diffusive processes, so there is a need for expanded studies of their effects.

Since the Gargett and Holloway and Gargett and Ferron parameterizations of double diffusion are rather simple, one must be concerned that their studies might overestimate the impact of differential mixing. There is good evidence that the double-diffusive processes are most active only under certain hydrographic conditions. Thus, as a next step in exploring the role of double diffusion, we review the scientific literature related to double-diffusive processes and propose a more realistic parameterization of double diffusion for OGCMs. This is applied in the climate-scale numerical model runs described below. However, the parameterization of mixing processes, both vertical and horizontal, requires careful treatment in numerical models. The oceanic circulation involves extremely broad scales in both time and space; thus, we can never resolve all the temporal and spatial scales in numerical models. Consequently, for the foreseeable future, subgrid-scale phenomena must be parameterized in ocean general circulation models. In fact, determining suitable parameterizations of subgrid-scale phenomena is one of the most critical problems in numerical modeling of the general circulation. Early ocean circulation models were mostly based on z coordinates, and subgrid-scale mixing was parameterized in terms of constant horizontal and vertical mixing. However, such simple horizontal/vertical mixing schemes can introduce strong artificial cross-isopycnal mixing near fronts, such as the Gulf Stream, where isopycnals slope sharply. To overcome the artificial cross-isopycnal mixing in low-resolution z-coordinate models, a numerical technique of rotating the mixing tensor has been proposed by Redi (1982) and has been implemented here.

In addition, Gent and McWilliams (1990, hereafter GM90) pointed out that there is an extra advection term in the tracer balance equation of non-eddy-resolving models, whose existence is due to the Lagrangian mean transport of mesoscale eddies. They introduced a parameterization based on a downgradient diffusion of the isopycnal layer thickness in adiabatic flow. The addition of this transport term makes the tracer conservation equations in a non-eddy-resolving model self-consistent and eliminates the unphysical background horizontal diffusion require in the earlier version of the isopycnal/diapycnal mixing schemes. The dynamic effect and model sensitivity on the isopycnal/diapycnal mixing have been discussed in several recent papers (Gent et al. 1995; Danabasoglu and McWilliams 1995).

In this study we will focus on the parameterization of diapycnal mixing in connection with double-diffusive processes. Based on results from theory, laboratory experiments, and oceanic observations, the intensity of double diffusion must depend on the local density ratio $R_\rho = \alpha T_z/\beta S_z$. There is strong evidence indicating that double diffusion is important in controlling the diapycnal mixing process in the ocean only if R_ρ is sufficiently close to one. Thus, we propose here a conservative parameterization of double diffusion that reflects this dependence (section 2). This parameterization is applied to the GFDL MOM2 (Pacanowski 1995) model. The numerical experiments and results are presented and interpreted in section 3. In addition, sensitivity study experiments are presented in section 4 in order to understand the response of the numerical model to the double-diffusive parameterization, and a summary follows in section 5.

2. Parameterization of double-diffusive processes

Double-diffusive convection can occur in a stably stratified environment where the vertical density gra-

dient due to either temperature or salinity is destabilizing. For the case with warm, salty water on top of cold freshwater, salt fingering occurs; for the case with cold freshwater on top of warm, salty water, diffusive layering appears (Turner 1973; Stern 1975; Schmitt 1994). Double diffusion occurs because of the two orders of magnitude difference in the molecular diffusivities of heat and salt. Double-diffusive mixing is driven by the release of potential energy in the redistribution of the destabilizing component, which has the larger buoyancy flux. A significant fraction of the released energy is used to move the stable component upward. However, the total density flux is downward, so the overall potential energy of the water column is reduced. As a result, double-diffusive processes are self-energized through the change in the mean potential energy. In the case of ordinary turbulent mixing, however, the potential energy of the water column is increased; thus external energy sources such as internal waves or strong mean shears are required.

Conditions favorable for double diffusion are very common in the oceans. In the subtropics the ocean gains heat from the atmosphere, and evaporation exceeds precipitation. Thus, in comparison with the deep ocean, the upper ocean is warm and salty, a stratification which favors salt fingering. Ingham (1966) reports that 90% of the main thermocline of the Atlantic Ocean has a density ratio less than 2.3. Schmitt (1990) finds that 95% of the upper kilometer in the Atlantic at 24°N is salt fingering favorable. In the western tropical North Atlantic an area of over 1 million km^2 was found to contain strong thermohaline staircases in the main thermocline (Schmitt et al. 1987). Systematic, large-scale water mass changes within the staircase layers were observed, which cannot be explained by conventional mechanical turbulence but fit nicely the enhanced salt flux expected from salt fingers. This location is characterized by a strong vertical salt gradient and a low value of the density ratio R_ρ. Microstructure observations (Gregg and Sanford 1987; Lueck 1987; Marmorino et al. 1987) revealed narrowband, limited amplitude structures of the predicted scale for salt fingers within the interfaces, and plumelike convective structures within the mixed layers. The intensity of the microstructure indicates that an eddy diffusivity for salt of 1–2 cm^2 s^{-1} must apply within the staircase (Schmitt 1988; Kunze 1990). While lower than expected from the simple application of laboratory flux laws, this is quite substantial compared to the weak background value of 0.07 cm^2 s^{-1} predicted for the canonical Garret and Munk (1972) internal wave field (Gregg 1989). Indeed, the vertical heat flux derived from the microstructure measurements is nearly 3 W m^{-2}, which exceeds the flux estimated in a very strongly turbulent, but weakly stratified, abyssal site near the Mid-Atlantic Ridge (Polzin et al. 1997). The salt finger mixing in this region of the Atlantic is thought to be responsible for the water mass conversion observed in the thermocline waters transiting from the South Atlantic to the Gulf Stream in the Florida Straits (Schmitz et al. 1993).

In addition to the strong vertical mixing inferred for the staircase regions such as the tropical Atlantic, Mediterranean outflow, and the Tyrhennian Sea, where the density ratio is less than 1.7, fingers are also thought to play some role in mixing in the broad central waters of the World Ocean, where the density ratio is only slightly higher. Some contribution is very likely since turbulence due to shear instability is infrequent, occurring only a few percent of the time (Polzin 1996). Laboratory experiments have shown that fingers grow rapidly after a turbulent mixing event, when the density ratio is near the common oceanic value of 2 (Taylor 1991). When fingers alone exist, there is a strong increase in laboratory fluxes as the density ratio drops below 2.0 (McDougall and Taylor 1984). Gargett and Schmitt (1982) find microscale signatures of fingers in the Central Waters of the North Pacific. Mack (1985, 1989) and Mack and Schoeberlein (1993) find salt finger signatures in microstucture data from the upper thermocline of the Sargasso Sea when the local density ratio falls below 3.0. Marmorino et al. (1987) also finds the distinct spectral signatures of salt fingers in data from the seasonal thermocline of the Sargasso Sea. Recent theoretical work of Shen and Schmitt (1995) provides a salt finger model spectrum that is in good agreement with the observed microstructure. It is based on the ''dispersion relation'' for salt fingers derived by Schmitt (1979), which shows that finger growth times are comparable to the local buoyancy period only when R_ρ is less than 2. Hamilton et al. (1989) report on salt finger signatures in microstructure data from the main thermocline of the eastern North Atlantic that appear to provide a significant vertical nutrient flux.

The extensive observational, laboratory, and theoretical evidence that fingers are most intense when the density ratio is less than about 2 leads us to propose a parameterization that is dependent on R_ρ. Schmitt (1981) has argued that the constancy of the large-scale density ratio observed in the main thermocline can be explained by this dependence and the greater transfer rate for salt. In the modeling below we adopt a parameterization similar to his [and to the form inferred by Kunze (1990)], though reduced in amplitude to conform with recent observations.

Due to surface cooling and excess precipitation, the surface water in polar and subpolar regions is colder and fresher than the subsurface water. As a result, the other type of double diffusion, diffusive convection (or layering), is possible. In this case, the heat content is the destabilizing component and more heat is mixed upward than salt. Though the initial process may appear as an oscillatory overstability (Stern 1960; Shirtcliffe 1967), the fully developed state is one of alternating convecting layers and high gradient sheets (Turner 1973); hence the name. The characteristic staircase layers have long been observed beneath the ice in the Arctic

Ocean (Neal et al. 1969; Neshyba et al. 1971). Padman and Dillon (1987, 1988) provide evidence for widespread diffusive staircases in both the Beaufort Sea and Canadian Basin. The Antarctic contains sites of strong diffusive layering as well. Muench et al. (1990) found numerous thermohaline staircases in the northwestern Weddell Sea during March 1986. Throughout an approximately 40 000 km^2 study area, they observed that between depths of 100 and 180 m, staircases with a typical scale of 1–5 m occurred almost everywhere. Between depths of 180 and 500 m, over ~50% of the study area were staircases with layer thickness of 10–100 m. Vertical heat fluxes of up to 15 W m^{-2} were estimated, which is significant in the upper-ocean heat budget and may help maintain ice-free conditions. Robertson et al. (1995) also found that diapycnal fluxes in the Weddell Sea were dominated by diffusive convection. Similarly, Martinson (1990) found it to be important in a model of winter sea ice formation. Kelley (1984, 1990) has provided a parameterization of the mixing due to diffusive convection, which derives from a successful scaling of the layer thicknesses in both the laboratory and ocean. Effective diffusivities are weaker than in the salt finger regime, consistent with the convective transports realized with fingers and the conductive fluxes obtained in diffusive interfaces.

In traditional numerical models diapycnal mixing in the stably stratified part of the model ocean is parameterized in terms of the same constant for both heat and salt. In this study we will divide the stably stratified region into three subregions:

1) salt fingering regime
2) diffusive layering regime
3) non-double-diffusive regime.

The convective adjustment scheme for regions of unstable stratification remains the same as in the normal MOM2 code.

a. Salt fingering regime

Salt fingers can form when warmer saltier water overlies colder fresher water such that

$$T_z > 0, \qquad S_z > 0, \qquad 1 < R_\rho < k_t/k_s, \tag{1}$$

where $R_\rho = \alpha T_z/\beta S_z$ is the density ratio, and k_t and k_s are the molecular diffusivities of heat and salt respectively. The ratio of molecular diffusivities is about 100, so a very weak destabilizing salinity gradient can induce salt fingering. However, observations indicate that fingers become significant mixing agents in the ocean only when the density ratio is close to unity (Schmitt 1994).

Here we apply the parameterization of Schmitt (1981)

$$K_S = \frac{K^*}{1 + (R_\rho/R_c)^n} + K^\infty$$

$$K_T = \frac{0.7K^*}{R_\rho[1 + (R_\rho/R_c)^n]} + K^\infty, \tag{2}$$

where K_S and K_T are the diapycnal eddy diffusivities for salinity and temperature, respectively; K^∞ is the constant diapycnal diffusivity due to other mixing processes unrelated to double diffusion, such as internal wave breaking, which is independent of R_ρ; and R_c is the critical density ratio above which the diapycnal mixing due to salt fingering drops dramatically, due to the absence of staircases. A value of 0.7 is used for the heat/salt buoyancy flux ratio due to salt fingers. Here K^* is the maximum diapycnal diffusivity due to salt fingers. We have chosen a more modest value than originally proposed by Schmitt (1981), reflecting improved understanding of fluxes in thermohaline staircases observed in the C-SALT program (Schmitt 1988). Exponent n is an index to control the decay of K_T, K_S with increasing R_ρ.

In numerical models, vertical gradients of temperature and salinity, T_z and S_z, are not well simulated compared to the oceanic observations. The simulation is especially poor in the deep ocean where the vertical gradients of temperature and salinity in low-resolution numerical models are very small and often noisy. On the other hand, most field observations of double diffusion are limited to the upper ocean, and it is not clear whether double diffusion can play any significant role at great depth where the vertical gradients of both temperature and salinity are small. Thus, we have introduced an additional constraint that double diffusion can occur only if the magnitude of the vertical temperature gradient is larger than a critical value:

$$|T_z| > T_{z,c}. \tag{3}$$

This is a conservative step to limit salt fingering to the thermocline, where evidence indicates its importance, and avoid it in the abyss, where such evidence is not yet available.

b. Diffusive layering regime

When

$$T_z < 0, \qquad S_z < 0, \qquad 1 > R_\rho > k_s/k_t, \tag{4}$$

diffusive layering can occur.

Kelley (1984) discussed a parameterization for diffusive layering process in which he applied the laboratory-derived double-diffusive flux laws to the oceanic data. The formulation is given as follows:

$$K_T = CR_a^{1/3}k_t$$

$$K_S = R_F R_\rho K_T, \tag{5}$$

where

$$C = 0.00859 \exp\{4.6e^{-0.54(R_\rho^{-1}-1)}\},$$

$$R_a = 0.25 \times 10^9 R_\rho^{-1.1}, \tag{6}$$

and k_t is the molecular diffusivity of heat; R_F is the buoyancy flux ratio defined as

$$R_F = \frac{\beta F_S}{\alpha F_T}, \tag{7}$$

in which F_S, F_T are upward flux of salt and heat respectively. Huppert's (1971) formulation for R_F has been used in Kelley (1984):

$$R_F = \begin{cases} 1.85 - 0.85/R_\rho, & 0.5 \le R_\rho < 1.0 \\ 0.15, & R_\rho < 0.5. \end{cases} \tag{8}$$

Roughly speaking, $K_S \approx K_T \approx 1.0$ cm^2 s^{-1} when $R_\rho \to 1.0$. Here K_S and K_T decrease approximately as R_ρ^4 and R_ρ^2, respectively, over the range $0.1 \le R_\rho \le 1.0$.

Furthermore, Kelley (1990) refined his formulation by giving a new empirical formulation of $C(R_\rho)$ and R_F:

$$C = 0.0032 \exp\{4.8R_\rho^{0.72}\}$$

$$R_F = \frac{1/R_\rho + 1.4(1/R_\rho - 1)^{3/2}}{1 + 14(1/R_\rho - 1)^{3/2}}. \tag{9}$$

Similar to the case of salt fingering, K_T and K_S are different and they depend on the density ratio. However, the diapycnal diffusivity suggested by Kelley (1984, 1990) was rather weak at low density ratios since K_S fell below the molecular diffusivity for heat (1.4×10^{-3} cm^2 s^{-1}) when $R_\rho < 0.25$, which could cause computational difficulty in a numerical model. On the other hand, given the role of non-double-diffusive processes in the diapycnal mixing (Muench et al. 1990), a background diffusivity is also needed in the region of diffusive layering. Thus, we include K^∞ in the parameterization for diffusive layering:

$$K_T = CR_a^{1/3}k_t + K^\infty$$

$$K_S = R_F R_\rho (K_T - K^\infty) + K^\infty, \tag{10}$$

where C and R_F are given in (9) and R_a defined in (6). Also, the restraint (3) is applied in the diffusive layering case as well. Note, however, the definition of density ratio in this paper is inverse to that in Kelley (1984, 1990) in order to deal with both forms of double diffusion. His formulation is quite conservative compared to that of Fedorov (1988) or Muench (1990), with weaker fluxes when R_ρ is close to 1.

c. Non-double-diffusive regime

Away from the regions discussed above, we use a constant background diapycnal mixing rate for both tracers to represent internal-wave-induced mixing:

$$K_T = K_S = K^\infty. \tag{11}$$

The sinking limb of the thermohaline circulation is driven by buoyancy losses at the air–sea interface; the return limb involves a balance between upward buoyancy advection and downward buoyancy diffusion in the ocean interior. However, in the GFDL MOM2, density is a diagnostic variable; thus the diapycnal eddy diffusivity of density K_ρ does not appear in the model explicitly. Instead, K_ρ is defined diagnostically as a function of the density ratio, assuming a locally linear equation of state applies to the mixing between adjacent layers. An expression equivalent to that given in GH92 is readily obtained:

$$K_\rho = \frac{R_\rho K_T - K_S}{R_\rho - 1}. \tag{12}$$

The change of diffusivities of temperature, salinity, and density with the density ratio is shown in Fig. 1, where we take the double-diffusive parameters as

$$K^* = 1.0 \text{ cm}^2 \text{ s}^{-1}, \qquad K^\infty = 0.3 \text{ cm}^2 \text{ s}^{-1},$$
$$R_c = 1.6, \qquad n = 6,$$
$$T_{z,c} = 2.5 \times 10^{-4}{}^\circ\text{C m}^{-1}. \tag{13}$$

Because heat and salt mixing rates are different, the equivalent buoyancy diffusivity varies greatly from one region to another (Fig. 1):

1) In the weak double-diffusive regime ($R_\rho < 0.3$ or $R_\rho > 3.0$), K_ρ is close to its upper limit, given by the constant turbulent mixing coefficient.
2) In the moderate double diffusion regime ($0.3 < R_\rho < 0.77$ or $0.97 < R_\rho < 1.0$ or $1.56 < R_\rho < 3.0$), K_ρ is reduced, so the mixing of buoyancy is less efficient.
3) In the strong double-diffusion regime ($0.77 < R_\rho < 0.97$ or $1.0 < R_\rho < 1.56$), the sign of K_ρ is reversed. Thus, upgradient buoyancy diffusion appears because the buoyancy flux due to the destabilizing component is larger than that of the stabilizing component.

3. Control experiments

a. The numerical experiments

The GFDL MOM2 is used in these experiments. The details of the model can be found in K. Bryan (1969) and Pacanowski (1995). The specific features of these experiments are as follows:

The model domain is a rectangular basin of 60° by 60°, and the horizontal resolution is 3.75°. There are 15 levels vertically, with thickness of 50 m, 75 m, 100 m, 125 m, 150 m, 200 m, 250 m, 300 m, 400 m, 450 m, 450 m, 450 m, 500 m, 500 m, and 500 m from the top to the bottom, and the total depth is 4500 m.

The annual zonally averaged climatological surface wind stress (Hellerman and Rosenstein 1993), SST, and SSS (Levitus 1982) are used in these experiments. The first layer temperature and salinity are relaxed to the SST and SSS climatology, with a relaxation time of 30 days.

The horizontal and vertical momentum viscosity coefficients are $A_h = 1.0 \times 10^{10}$ cm^2 s^{-1} and $A_v = 20$ cm^2 s^{-1} respectively. For the tracer equations, the eddy transport parameterization of GM90 and isopycnal/diapycnal

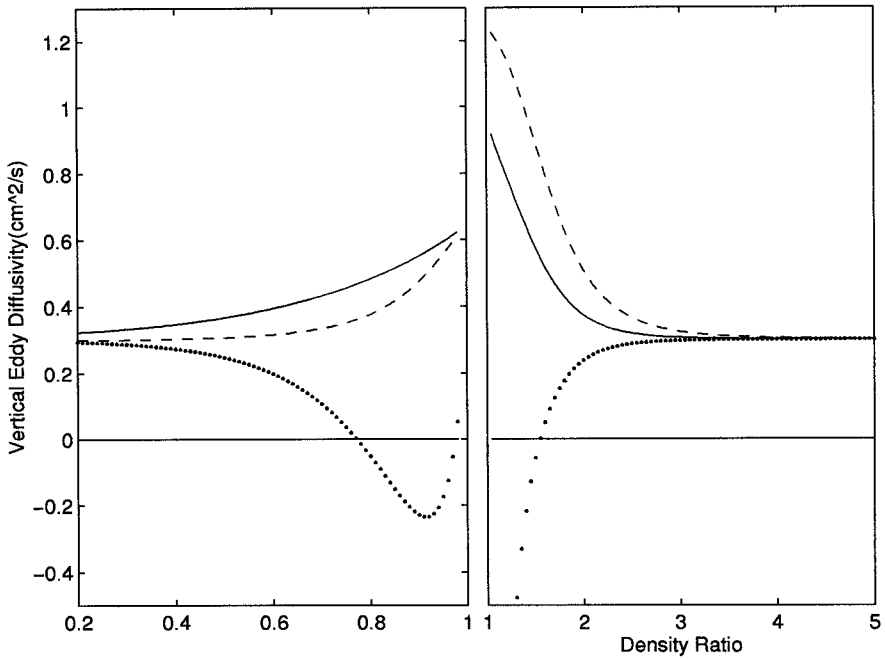

FIG. 1. The change of diapycnal eddy diffusivities of temperature (solid line), salinity (broken line), and density (dotted line) with density ratio R_ρ. In the left half panel, where $R_\rho < 1$, diffusive layering mixing occurs. In comparison, in the right half panel where $R_\rho > 1$, salt fingers form. Note that even though diffusive layering region and salt fingering region seem to be continuous at $R_\rho = 1$, in the real ocean, normally there is a gravitationally unstable transition region between them where $R_\rho < 0$.

mixing is used, and no background horizontal diffusion is needed. We take $K_{\rm ISO} = K_{\rm ITD} = 5 \times 10^6$ cm^2 s^{-1}, where $K_{\rm ISO}$ is the isopycnal diffusion coefficient and $K_{\rm ITD}$ is the downgradient diffusivity of the isopycnal thickness.

Three control experiments will be discussed here, the first with the double-diffusive parameterization (DDP hereafter) for temperature and salinity, and the second with the diffusivity given in a similar fashion to GH92 (Gargett and Holloway diffusivity, GHD hereafter), that is, the diffusivities for heat and salt are different but both kept constant everywhere, and the third with the conventional assumption of $K_S = K_T =$ const, (constant diapycnal diffusivity, CDD hereafter). Gargett and Holloway (1992) discussed many experiments in their paper, but given the differences in the formulation of the numerical model, particularly the inclusion of GM90, we deemed it worthwhile to run an experiment similar to theirs and to compare the results directly.

The parameters in the double-diffusion parameterization are defined in (13). Note that this parameterization is more conservative than that of Schmitt (1981). This is adopted because results of the C-SALT observations (Schmitt 1988) indicate that a modest reduction of the mixing coefficient was appropriate. The uncertainties associated with these parameters and vertical resolution will be discussed in detail in the next section.

We designed these three experiments in such a way that everything is identical except for the parameterization of diapycnal diffusion. All experiments run from the same initial conditions and under the same boundary conditions for 8000 years. For the reason of comparability, we calculate the basin-averaged K_T and K_S in run DDP: $\overline{K_T} = 0.326$ cm^2 s^{-1} and $\overline{K_S} = 0.366$ cm^2 s^{-1}, and then we use $K_T = 0.326$ cm^2 s^{-1} and $K_S = 0.366$ cm^2 s^{-1} in run GHD and $K_T = K_S = 0.346$ cm^2 s^{-1} in run CDD; therefore the average diffusivities of both scalars are equal in all three experiments.

A technical issue is the computational cost of adding on the double-diffusive parameterization. For a 100-yr integration on an SGI workstation, the CPU time is 1256, 1120, and 1113 CPU seconds for runs DDP, GHD, and CDD respectively. Thus, the double-diffusive parameterization takes approximately 10% extra computational time, a rather modest cost.

b. Results and interpretations

1) DIFFUSIVITY VARIABILITY IN RUN DDP

The major difference between DDP and GHD/CDD is that K_T and K_S in run DDP depend on the spatial variability of density ratio R_ρ. It is found that salt fingers are the dominant double-diffusive phenomenon; thus, here we only map out the distribution of the salt dif-

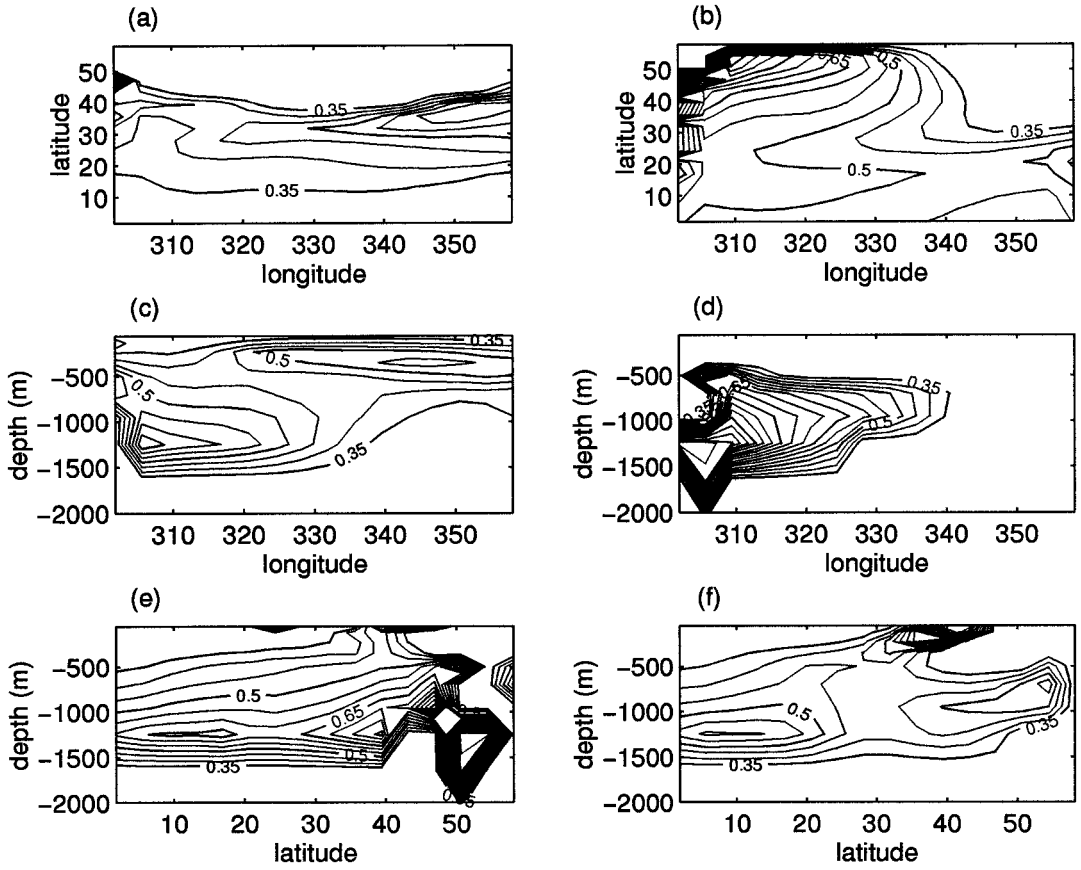

FIG. 2. The K_S distribution in run DDP of different sections: (a) horizontal section in the upper thermocline (350 m); (b) horizontal section in the lower thermocline (950 m); (c) zonal section in the subtropical gyre (32°N); (d) zonal section in the subpolar gyre (50°N); (e) meridional section close to the western boundary (305°E); and (f) meridional section in the interior (334°E). The contour interval is 0.05 cm^2 s^{-1}.

fusivity and the corresponding K_T distribution can be deduced accordingly.

To visualize the complicated three-dimensional structure of the circulation we plot several two-dimensional maps of K_S in Fig. 2.

There are two distinct features in the K_S distribution:

1) The double diffusion is confined within the upper 1500 m; thus only the upper 2000 m are plotted in Figs. 2c–f. Double diffusion is stronger near the bottom of the thermocline (e.g., 950 m in Fig. 2b) than in shallower layers (e.g., 350 m in Fig. 2a). The lack of double-diffusive activity in the deep part of the model ocean is due to the temperature gradient constraint (3), which eliminates the double-diffusive processes in the deep ocean where the vertical gradients in the numerical model are weak. This constraint also reflects that we have no reliable observational data to support double-diffusive phenomena in the deep ocean. Such a constraint can be modified in the future based on new observations.
2) In the western boundary region K_S is stronger than in the interior, indicating strong salt fingering there. The enhanced salt fingering is associated with strong vertical salinity gradients within the western boundary region. According to the classic picture of the oceanic general circulation there are surface and deep western boundary currents. The surface western boundary current brings warm and salty water northward, and the deep western boundary current brings cold and fresh water southward along the western boundary. As a result, the temperature and salinity distributions within the western boundary region are dominated by horizontal advection, which maintains strong vertical gradients of salinity along the path of the western boundary currents, and this is the region most favorable for salt fingering because R_ρ is brought closer to 1. In comparison, vertical diffusion may play a more prominent role in the oceanic interior, thus limiting the vertical gradient of salinity there. As a result, salt fingering in the ocean interior is not as strong as within the western boundary region where vertical shear between poleward and equatorward water masses maintains the salinity contrast.

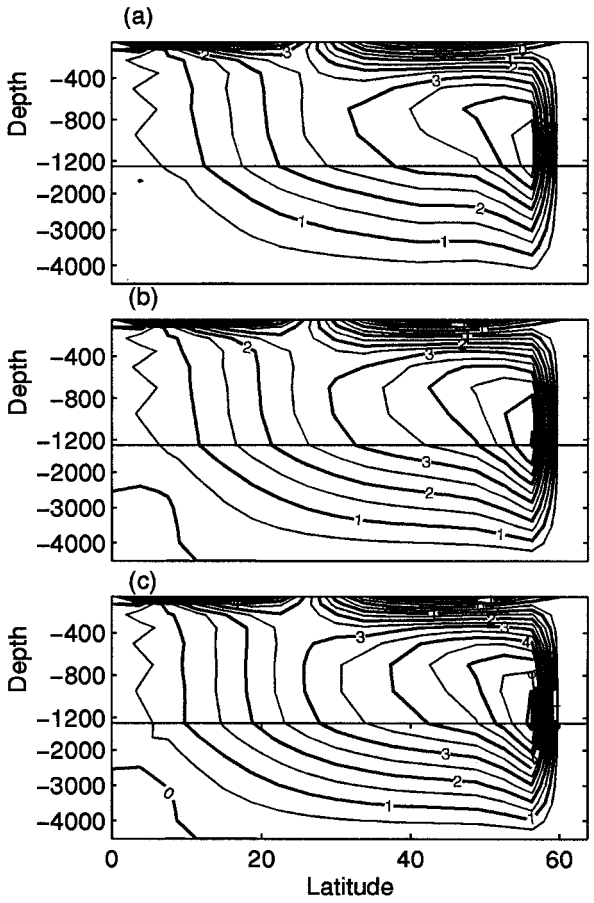

FIG. 3. The zonally integrated meridional overturning volume streamfunctions for run (a) DDP, (b) GHD, and (c) CDD. Contour interval is 0.5 Sv.

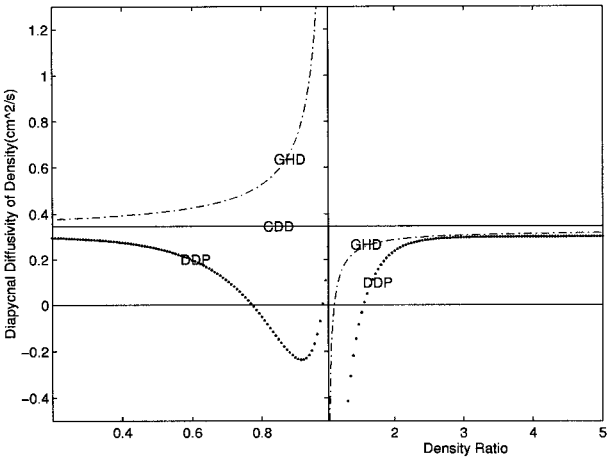

FIG. 4. Relation between K_ρ and R_ρ in the three different experiments.

2) MERIDIONAL OVERTURNING

The thermohaline circulation can be visualized by plotting the zonally integrated meridional overturning streamfunction. The structure of the thermohaline circulation in the three cases (Fig. 3) is similar, but the magnitudes are significantly different. The overturning rate in run CDD is 6.17 Sv (1 Sv $\equiv 10^6$ m^3 s^{-1}); while it is only 4.79 Sv in run DDP, a 22% decrease compared with run CDD. In run GHD the meridional overturning is 5.55 Sv, a 10% decrease compared with run CDD. There are traces of two-grid noise near the equator in all three experiments, which may be due to the coarse vertical resolution (Weaver and Sarachik 1990). In addition, a very weak reversed meridional cell in the equatorial deep ocean appears in run GHD and CDD. However, there is no reversed cell in DDP, and this may be due to the fact that the double-diffusion parameterization helps to eliminate the local water column instability, which leads to the local reversed cell.

According to the classic Stommel–Arons theory (Stommel and Arons 1960), deep water moves equatorward as a deep western boundary current after its formation at high latitudes. The deep water returns to the source region through basinwide uniform upwelling in the ocean interior. To reach an equilibrium, the diapycnal advection (upwelling) must be compensated by the diapycnal diffusion. Thus, the magnitude of the thermohaline circulation is very sensitive to the diapycnal diffusivity of density, as shown by F. Bryan (1987).

Given the importance of the diapycnal diffusivity of density, we plot the relation of K_ρ and R_ρ in Fig. 4. In run CDD, $K_\rho = K_S = K_T$ is constant; however, in run GHD and DDP, K_ρ depends strongly on R_ρ. In the region of diffusive layering ($R_\rho < 1$), K_ρ in run GHD is larger than the constant K_T and K_S specified in the experiment. This is contrary to the common belief that diffusive layering reduces or even reverses the vertical buoyancy diffusion, as in run DDP. In GH92, this drawback was avoided by giving $d = K_S/K_T > 1$ or $d = K_S/K_T < 1$ according to whether salt fingering or diffusive layering is favorable; thus, in both regimes K_ρ is either reduced or with the sign reversed, in accordance with double-diffusive processes.

In the experiments studied here, salt fingering is the dominant double-diffusive process; therefore, only a very small region in run GHD is affected by an unphysical representation of the diffusive layering process. The circulation is primarily controlled by salt fingering, and the relation between the density ratio and density diffusivity is plotted in the right half of Fig. 4. We can see that both GHD and DDP are consistent with the fingering mechanism while displaying significant quantitative differences. First of all, given the same R_ρ, K_ρ is largest in run CDD, and then GHD, and smallest in run DDP. This difference increases when R_ρ is closer to 1. As we will discuss later, the implementation of a double-diffusive parameterization has an effect on the distribution of density ratio (Turner angle), which leads to a wider area of double-diffusively favorable conditions. Thus, we can imagine that the difference between

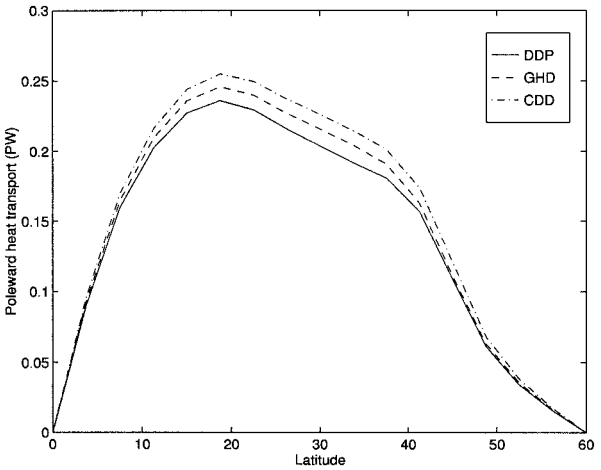

FIG. 5. The poleward heat transport for the three experiments.

the model runs may be greater than the diffusivity differences at the same R_ρ.

Since downward buoyancy diffusion in run DDP is weaker than in runs GHD and CDD, a smaller amount of upwelling is needed to balance the weaker density diffusion. Thus, the magnitude of the thermohaline circulation in run DDP is reduced. Furthermore, upwelling is not spatially uniform. In fact, upwelling within the western boundary region is two orders of magnitude stronger than in the interior in all the runs (Huang and Yang 1996); thus, upwelling within the western boundary region constitutes an essential part of the upward limb of the thermohaline circulation. As discussed in section 2, when double diffusion is sufficiently strong (R_ρ close to 1), buoyancy diffusion is reduced or reversed. Strong double diffusion in the western boundary region (Fig. 2) dramatically reduces the downward buoyancy diffusion and can reverse its direction locally. Even though diapycnal diffusion in the ocean interior is less affected, the total amount of the diapycnal diffusive flux of buoyancy is reduced and, therefore, the thermohaline circulation becomes weaker.

3) POLEWARD HEAT TRANSPORT

With significant changes in the magnitude of the thermohaline circulation, it is not surprising that the poleward heat transport is also affected by the different parameterizations of diapycnal processes (Fig. 5). The poleward heat transport at all latitudes is weakest in run DDP and strongest in run CDD, while it is intermediate in run GHD. The difference in poleward heat flux is most significant at midlatitudes. The maximum poleward heat flux in run CDD is 0.255 PW, and it is 0.246 PW in run GHD and 0.236 PW in run DDP, a 4% and 8% decrease respectively. Note that the decrease in the heat transport is less than the decrease in the thermohaline circulation. This can be explained as follows. First, the poleward heat transport is proportional to the meridional overturning rate multiplied by the temperature difference between the surface and deep water. While the maximum of the thermohaline circulation lies at high latitudes, the largest surface−deep water temperature difference appears at lower latitudes. Thus, the maximum poleward heat transport is found in midlatitudes, where the percentage of reduction of the thermohaline circulation at that latitude is less than that of the maximum overturning rate, and the temperature difference remains nearly the same for two experiments. Second, the wind-driven gyre and Ekman cell also contribute to the poleward heat transport; these are controlled by the surface wind stress and remain almost the same for both experiments.

4) TURNER ANGLE

Since R_ρ can vary from $-\infty$ to ∞ and it cannot represent the convective overturning regime, we would like to describe the spatial structure of the density ratio by mapping the Turner angle (Tu). Ruddick (1983; 1996 personal communication) defined the Turner angle as the four quadrant arctangent of R_ρ, that is,

$$\mathrm{Tu} = \arctan\left(\frac{R_\rho + 1}{R_\rho - 1}\right). \tag{14}$$

Thus, salt fingering occurs for $45° < \mathrm{Tu} < 90°$, and it is strongest when Tu is close to 90°. In comparison, diffusive layering occurs for $-90° < \mathrm{Tu} < -45°$ and when Tu is close to −90°, diffusive layering is strong. When $-45° < \mathrm{Tu} < 45°$, the fluid is in the non-double-diffusive regime. Other Tu values are within the gravitationally unstable region.

The Turner angle maps from the three experiments are complex; Tu at level 7 (950 m) and level 13 (3500 m) is plotted in Fig. 6. Differences among the three experiments are obvious: (i) Near the bottom of the thermocline (level 7), salt fingering favorable conditions are found in all experiments. Interestingly, the Tu in run DDP is highest, and then run GHD, and lowest in run CDD, indicating that salt finger mixing in DDP is reinforced, especially near the western boundary current (WBC). This also occurs in run GHD, though not as strongly as in run DDP. (ii) In the deep ocean (level 13), the Turner angle is only marginally critical in limited regions in run CDD, but salt fingering (in the subtropical gyre) and diffusive layering (in subpolar gyre) both occur in run DDP. In run GHD, however, only the salt fingering favorable condition is found, and it is weaker than in run DDP.

Thus, double diffusion appears to change the distribution of the Turner angle. In these model runs, this parameterization renders the water column even more favorable to double diffusion. Although both salt fingering and diffusive layering are possible in run DDP, strong salt fingering appears over most of the basin, while diffusive layering is confined to narrow regions

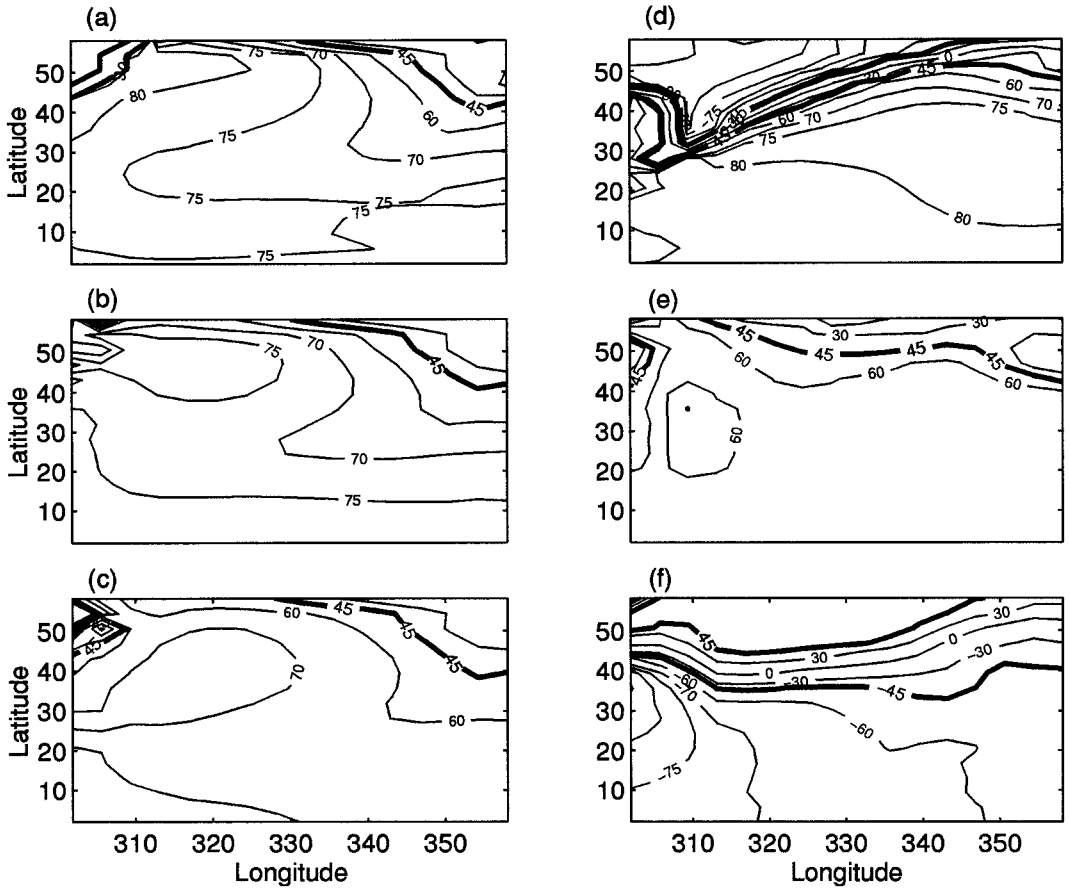

FIG. 6. The Turner angle at the bottom of level 7 (950 m) for run (a) DDP, (b) GHD, (c) CDD and at the bottom of level 13 (3500 m) for run (d) DDP (e) GHD, and (f) CDD respectively. Note that uneven contour intervals have been used in the above figure.

in the subpolar gyre near the surface or close to the bottom. The simple representation of double diffusion in GHD makes the deep water more salt fingering favorable but eliminates the regime for diffusive layering as in run DDP and CDD.

The density ratio is the most important index for double-diffusive activity. It controls the intensity of double diffusion and thus affects the large-scale thermohaline circulation and water mass formation (see next). For both double-diffusive runs, we found that the distribution of density ratio in the upper kilometer at 24°N was in better agreement with the hydrographic data for the Atlantic as reported by Schmitt (1990) than the constant diffusivity run. However, the improvement was small since the relaxation boundary conditions play a dominant role in setting upper-ocean *T–S* structure. We find that the addition of double diffusion causes the density ratio to become closer to one, which is somewhat counterintuitive (Fig. 6). This means that double-diffusive processes and large-scale circulation interact in a complicated way. Double diffusion in a one-dimensional (vertical) situation cannot be self-enhancing because of the weakening of the destabilizing gradient, which would shift R_ρ away from one (Schmitt 1981). However, in a two- or three-dimensional model, double-diffusive activity can reinforce itself. The double-diffusive lateral intrusions described by Turner (1978), Ruddick and Turner (1979), and Ruddick (1992) are a clear example of such self-reinforcing flows. That is, the maintenance and intensification of the double-diffusively favorable density ratio are due to the action of vertical shear on isopycnal gradients. The shear arises from horizontal pressure gradients developed when the double-diffusive fluxes begin affecting the vertical density profile. Whereas thermohaline intrusions have vertical scales of 100 m or less, it appears that such effects occur with much larger vertical scale within our model as well, based on the comparison of the DDP and CDD runs. As there are 1000-m vertical-scale water masses in the ocean with similarly low density ratios, it would be interesting to determine how much of it is due to self-enhancing effects versus the juxtaposition of shear and isopycnal

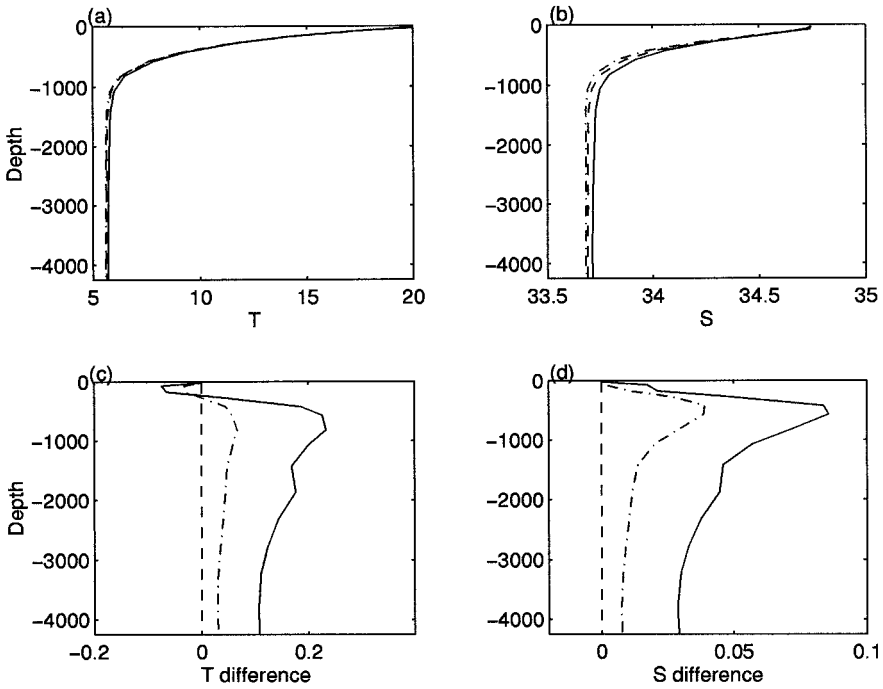

FIG. 7. Vertical profiles of horizontally averaged (a) temperature and (b) salinity, respectively, where the solid line is for run DDP, the dotted broken line for run GHD, and the broken line for run CDD. The difference from run CDD of (c) temperature and (d) salinity respectively.

gradients due to the wind- and buoyancy-driven circulations.

5) TEMPERATURE AND SALINITY DISTRIBUTION

The double-diffusive parameterization is also found to affect the basinwide water mass properties. Changes in the temperature and salinity distribution due to DDP can be seen from the horizontally averaged temperature and salinity profiles (Fig. 7). Compared to run CDD, the basin-averaged temperature in run DDP and GHD is lower in the uppermost 200 m, while it is higher below 200 m. On the other hand, the horizontally averaged salinity in both DDP and GHD is higher for the whole water column. The difference from run CDD is similar for run GHD and DDP, and both display the most significant differences in the main thermocline. On the other hand, the difference from CDD seems twice as large in run DDP as in run GHD for the whole depth. The basin averaged temperature is 6.069°C for run DDP, 5.973°C for run GHD, and 5.937°C for run CDD, and the salinity is 33.749 psu, 33.723 psu, and 33.711 psu, respectively; thus, water in run DDP is 0.13°C warmer and 0.04 psu saltier than in run CDD, while it is 0.04°C warmer and 0.01 psu saltier in run GHD compared to run CDD.

Tracer distributions are controlled by advection and diffusion. While the wind-driven horizontal advection plays a prominent role in setting up the tracer distribution in the upper ocean, tracer distributions below the main thermocline are dictated by vertical advection and vertical diffusion with the horizontal advection playing a minor role only.

Under the relaxation conditions for both temperature and salinity, surface temperature and salinity are nearly fixed to their climatological mean values. Since the salinity diffusivity in run DDP and GHD is larger than in run CDD, salinity is higher due to stronger downward salt diffusion in both DDP and GHD, compared with CDD, as shown in Fig. 7.

Changes in the temperature profile can be explained by a simple one-dimensional advection–diffusion balance, neglecting the lateral advection and diffusion terms. That is, the temperature distribution is controlled by the following one-dimensional balance $wT_z = \kappa T_{zz}$, where z is the distance along the path connecting the cold source and the hot source. Assuming both w and κ are constant along the path, the solution of this one-dimensional equation is in form of $T = T_1 + C(T_2 - T_1)(e^{az} - 1)$, where $C = 1/(e^{aD} - 1)$ in which D is the distance between the cold and hot source and $a = w/\kappa$ is the inverse of the characteristic scale of this advection–diffusion problem. Small a means a diffusion-dominated case, with almost a linear profile between the cold and heat source, while large a indicates a sharp front, like the main thermocline.

Salt mixing (circulation) is stronger (weaker) in run DDP and GHD, compared with CDD. Thus, the salinity profile in these two cases should have a broad halocline, thus a high salinity in the abyssal water. From this so-

TABLE 1. Parameter sensitivity experiments and results.

K^* (cm^2 s^{-1})	R_c	n	THC (Sv)	K_T (cm^2 s^{-1})	K_S (cm^2 s^{-1})
1.0	1.6	6	4.793	0.326	0.366
0.0	1.6	6	5.578	0.300	0.300
0.2	1.6	6	5.505	0.304	0.310
0.5	1.6	6	5.137	0.311	0.329
2.0	1.6	6	4.156	0.350	0.426
5.0	1.6	6	3.475	0.379	0.506
1.0	1.2	6	5.245	0.305	0.313
1.0	2.0	6	3.935	0.356	0.441
1.0	1.6	2	3.759	0.353	0.436
1.0	1.6	12	5.252	0.310	0.323
1.0	1.6	32	5.310	0.306	0.313
2.0	1.2	6	5.176	0.327	0.351
0.5	2.0	6	4.650	0.329	0.375

lution, it is clear that strong diffusion and weak circulation give rise to a broad main thermocline and warm and salty abyssal water, as shown in Fig. 7.

The temperature profile is slightly more complicated to explain. In run DDP, strong mixing above the bottom of the main thermocline transports more heat downward, so temperature is higher in the main thermocline, as shown in Fig. 7. Warm water in the main thermocline makes the water in the whole basin warmer than in run CDD, even though thermal diffusion below the main thermocline in run DDP is weaker than in run CDD. The shallow cold temperature anomaly near the surface in run DDP reflects that thermal diffusion there is lower than average.

The temperature profile in run GHD is the result of a delicate balance between a weakened circulation and weakened diffusion. Compared with run CDD, the circulation in run GHD is 10% weaker and diffusion is 5% weaker. Thus, the characteristic scale $1/a$ is reduced, and diffusion becomes more important than advection. As a result, the main thermocline is slightly broader, thus the warm anomaly compared with run CDD, as shown in Fig. 7.

4. Sensitivity experiments

Although the parameterization of double diffusion used here is consistent with existing theoretical, laboratory, and observational results, the parameterization involves several free parameters. Therefore, it is important to test the sensitivity of the model runs to these parameters as well as other specifics of the numerical model, such as the vertical resolution. Note that all parameters in these experiments are the same as in run DDP unless stated otherwise.

a. Parameter sensitivity

There are four variables in the parameterization given in section 2: K^*, K^∞, R_c, and n. One special feature of this parameterization is that diapycnal mixing consists of two parts: one part accounts for the double-diffusive processes and the other part, K^∞, represents the conventional, non-double-diffusive mixing due to turbulence (from internal wave breaking). The magnitudes of both K^* and K^∞ are not firmly established, and it is worthwhile to examine the sensitivity of the model to the ratio K^*/K^∞. For simplicity, we fix $K^\infty = 0.3$ cm^2 s^{-1} and change the value of K^*.

This background diffusivity is higher than the value inferred from the tracer release experiment of Ledwell et al. (1993), which suggested a diffusivity of 0.15 cm^2 s^{-1} in the main thermocline (which may be partially explained by salt fingers). As Yin and Fung (1991) have shown, unphysical vertical mixing in models with uneven vertical grids may occur, if the diffusivity is low, and this contaminates the numerical results. In order to avoid such numerical problems in our low-resolution experiments, we have used a slightly high value of 0.3 cm^2 s^{-1}, which represent a compromise among the affordable vertical resolution, isopycnal mixing rate, and the observations. Therefore, we only need to test three parameters, and the experiments and results are summarized in Table 1.

From Table 1 we can see that different parameters can lead to very different results. When we increase K^*, that is, the contribution from the double-diffusive part, both $\overline{K}_T$ and $\overline{K}_S$ increase in a quasi-linear fashion and the increase of double-diffusive processes decreases the diapycnal diffusion of density; thus the magnitude of the meridional overturning is reduced. Similarly when we increase R_c or decrease n, allowing modest fingering to affect a greater portion of the water column, the mean diffusivity for heat and for salt increases and the thermohaline circulation weakens.

The relationship between R_ρ and the eddy diffusivities for salt and heat is still not fixed. Schmitt (1981) applied the laboratory-derived flux laws to the observational data and estimated the eddy diffusivities for salt and heat. The maximum diffusivity due to salt fingers could reach 5.0 cm^2 s^{-1} or more, however, given the uncertainty associated with the empirical flux laws and more understanding gained through the C-SALT (Schmitt et

TABLE 2. $T_{z,c}$ sensitivity experiments and results.

$T_{z,c}$ (10^{-4}°C m^{-1})	THC (Sv)	K_T (cm^2 s^{-1})	K_S (cm^2 s^{-1})
0.0	4.733	0.386	0.476
1.0	4.749	0.337	0.389
2.5	4.811	0.326	0.366
5.0	4.861	0.323	0.360
10.0	4.944	0.318	0.348

al. 1987) field program, we judged that a good first step was to use a somewhat conservative value for K^*, like $K^* = 1.0$ cm^2 s^{-1}. As even this conservative value leads to a marked difference in the thermohaline circulation, it suggests that more work should to be done to understand the role of salt fingers in oceanic mixing.

Both R_c and n affect the relation among K_T, K_S, and R_ρ, and little is known about the exact value of them. However, on the basis of the limited observational data, K_S appears to be large for R_ρ less than 1.5, falling dramatically near $R_\rho = 1.7$ and reaching background levels by $R_\rho = 1.9$. Thus, $R_c = 1.6$, $n = 6$ are reasonable based on observation. Even though the theoretical condition for salt fingers is $1 < R_\rho < 100$, observational data suggests that significant fingering only occurs when R_ρ is close enough to 1. A similar conclusion holds for the diffusive layering. Therefore, a relatively stronger vertical gradient of salt (temperature) is required for the salt fingering (diffusive layering) to be important in the diapycnal mixing processes.

b. Sensitivity to restraint $T_{z,c}$

Experiments and results with different $T_{z,c}$ are summarized in Table 2. The magnitude of $T_{z,c}$ can make a significant difference in basin-averaged diffusivities for salt and heat, while the magnitude of meridional overturning remains nearly the same. The reason is that the effect of the constraint $T_{z,c}$ works like a filter: it only affects the part of ocean below the main thermocline where the vertical gradients of temperature and salinity are weak. In the main thermocline, however, T_z is much larger than the $T_{z,c}$ given in the above table, and thus the double diffusion in the main thermocline remains almost the same. As found by Cummins et al. (1990), an increase of diffusivity in the deep ocean (they use a diffusivity that is inversely dependent on the local buoyancy frequency) increases the vertical gradient of T, S in the deep ocean, but the magnitude of the thermohaline circulation is barely changed.

The criteria of a minimum $T_{z,c}$ for double diffusion to occur is speculative. We viewed it as a way to avoid spuriously large double-diffusion in the weakly stratified abyss, where there is little evidence for its importance, and noise in the computation of vertical gradients might be a problem.

Even though the double-diffusive activity in the deep ocean does not affect the magnitude of thermohaline circulation much, it can make a significant difference in the distribution of temperature and salinity. In comparing a DDP run with $T_{z,c} = 0.0$ to a CDD experiment with $K_T = K_S = 0.43$ cm^2 s^{-1} (the mean diffusivity in the DDP run), we find that the temperature is lower in the main thermocline (0–500 m) and warmer below 500-m depth, and the salinity is higher for the whole water depth. These changes in water mass properties caused by the double diffusion are of interest for climate studies. We do not intend to compare results from our idealized runs with observations. However, we hope that the underlying dynamics should apply to the more practical and complicated climate models. Danabasoglu and McWilliams (1995, DM hereafter) have tested the sensitivity of a global ocean circulation model to parameterizations of mesoscale isopycnal tracer transports and showed substantial improvement in several climatically important aspects of the ocean circulation, compared with the conventional horizontal/vertical eddy diffusion parameterization. However, the horizontally averaged temperature is warmer in the main thermocline and colder in the deep ocean compared with Levitus data (Levitus 1982) in their model (refer to Fig. 8 in DM). The salinity is fresher throughout the water column, especially in the deep ocean (refer to Fig. 16 in DM). These discrepancies are just the opposite of the changes we see in our $T_{z,c} = 0$ run. Thus, our results suggest that the vertical temperature and salinity distributions could be improved in such global climate models if a parameterization of double diffusion were to be applied in the deep ocean. In this regard we note that McDougall and Whitehead (1984) invoked some salt fingering to explain the evolution of water mass properties in the Antarctic Bottom Water in the Atlantic.

c. Salt fingering and diffusive layering alone

To study the different roles played by salt fingers and diffusive layering in run DDP, we ran two experiments in which these processes are separated with only one of them active in each experiment. For example, in the salt fingering alone run, the salt fingering parameterization (2) is activated, but diffusive layering is shut off; that is, a constant $K_T = K_S = K^\infty = 0.3$ cm^2 s^{-1} is applied in places with no salt finger activity. The experiment for diffusive layering only is designed similarly.

In the salt fingering alone experiment, the meridional overturning rate is 4.80 Sv, and the globally averaged diffusivities are $\overline{K}_T = 0.325$ cm^2 s^{-1} and $\overline{K}_S = 0.366$ cm^2 s^{-1}, which is very close to run DDP. In contrast,

in the diffusive layering alone experiment the meridional overturning rate is 5.58 Sv, and both $\overline{K}_T$ and $\overline{K}_S$ is no more than 0.0003 cm^2 s^{-1} higher than K^∞. Therefore, diffusive-layering activity is barely noticeable in these runs. Even though changes in K_T and K_S are almost trivial, the meridional overturning rate is enhanced compared to the overturning rate of 5.575 Sv for the case with $K^* = 0$, as shown in Table 1. This result implies that diffusive layering may tend to intensify the thermohaline circulation. This might occur because the process can release heat to the upper ocean without experiencing deep convection, thereby converting a warm, salty water mass to a cold, salty water mass that more readily sinks. McDougall (1983) invokes such a mechanism for Greenland Sea Bottom Water formation. However, for our model, the effect is small, possibly because of the 60° northern limit to the domain and the lack of an Arctic Ocean, where the most extensive diffusive layering is found (Padman and Dillon 1988).

Both experiments show that under restoring boundary conditions, salt finger mixing occurs much more widely than diffusive layering. The additional constraint on $T_{z,c}$ could eliminate some places where diffusive layering is possible due to weak T_z, but the fingers predominate largely because of the restoring boundary conditions and the deep water formation at high latitudes, which produces cold, fresh deep waters. Thus, under such upper boundary conditions, diffusive mixing plays a small role in the diapycnal diffusion. In this case, the unphysical representation of diffusive layering by a simple $d = K_S/K_T > 1$ in experiment GHD does not affect the result too much.

However, if we use a virtual salt flux condition or natural boundary condition (Huang 1993), the situation should be different. Under the so-called mixed boundary conditions, multiple equilibria exist. Convection could happen near the equator rather than in the polar region in the hemisphere model, or sinking near one pole while upwelling near another pole in a global model, thus the conditions favorable for diffusive layering are not affected in places where no convection occurs, and then it may be essential for the diapycnal mixing processes.

d. Sensitivity to the vertical resolution

The strength of double-diffusion activity depends on the density ratio, $R_\rho = \alpha T_z/\beta S_z$, which involves the vertical gradient of temperature and salinity. Vertical temperature and salinity gradients may be poorly simulated in low-vertical resolution models. In addition, the vertical layer scale of staircases observed is smaller than the vertical grid scale (which produces the necessity for a parameterization). Thus, a natural question is how sensitive is the parameterization to the vertical resolution.

We ran an experiment with a doubled vertical resolution (compared to run DDP) and kept all other parameters the same. The meridional overturning cell in this new experiment is 5.02 Sv, and the basin-averaged diffusivities are $\overline{K}_T = 0.337$ cm^2 s^{-1}, $\overline{K}_S = 0.388$ cm^2 s^{-1}. Compared to run DDP, it is clear that both the thermohaline circulation and basin-average mixing rates $\overline{K}_T$, $\overline{K}_S$ intensified.

The increase of the strength of the thermohaline circulation can be attributed to two aspects: (i) The increase of vertical resolution alone can increase the magnitude of the thermohaline circulation. We ran two experiments with constant $K_T = K_S = 0.45$ cm^2 s^{-1}, one with 15 vertical levels and another with 30 levels. The meridional overturning rate was 7.47 Sv and 7.64 Sv respectively, with a small difference of 0.17 Sv. Thus, we can expect a similar effect in the DDP experiments. (ii) Even though the averaged K_T, K_S are larger for the case with the higher vertical resolution, the strength of double diffusion in the main thermocline is actually slightly lowered. Since the increase of vertical resolution can increase the vertical gradient of temperature and salinity (Weaver and Sarachik 1990), especially in the deeper parts of the ocean, double diffusion can occur in this experiment at places where T_z is lower than $T_{z,c}$ in the standard DDP run. Examination of the vertical distribution of diffusivities reveals that double diffusion reaches deeper in the experiment with higher vertical resolution than in the standard run. Thus, an increase in vertical resolution can improve the distribution of water masses, but the meridional overturning rate remains almost unchanged.

5. Summary

An investigation of the effects of double-diffusive mixing on the general circulation has been carried out using a more realistic parameterization than that used by Gargett and Holloway (1992), who applied a universal nonunity ratio between the vertical diffusivities of heat and salt. The parameterization has three distinct features compared with the conventional constant eddy diffusivity assumption: 1) The vertical eddy diffusivities of temperature (K_T) and salinity (K_S) are different. For salt finger mixing, $K_S > K_T$, and vice versa for diffusive layering. 2) Both K_T and K_S increase when the local density ratio $R_\rho = \alpha T_z/\beta S_z$ is close to 1, and there is a cutoff in the R_ρ dependence. 3) A constant diapycnal diffusivity applies for non-double-diffusive turbulent mixing. When $R_\rho > 3.0$ or $R_\rho < 0.3$, the diapycnal diffusivity is dominated by turbulent mixing rather than double diffusion. This conservative implementation of a double-diffusive parameterization leads to a decrease of the downward buoyancy diffusion.

Three experiments have been carried out using the GFDL MOM2 code based on standard relaxation boundary conditions for the surface temperature and salinity. The first run applied the above parameterization (DDP), the second run used the GH92 parameterization (GHD), and the third run used a constant diapycnal diffusivity (CDD). Compared to run CDD,

the meridional overturning rate in run DDP is reduced by 22% because of the reduced buoyancy flux, and the poleward heat transport is reduced by 8%. In comparison, the corresponding decrease in run GHD is 10% and 4% respectively. The density ratio distribution in run DDP and GHD is more favorable for double diffusion than in run CDD, indicating that changes in buoyancy fluxes affected the pressure field in a way that enhances the differential advection of heat and salt. Note that changes in the density ratio distribution in run DDP are larger than in run GHD. Finally, deep temperatures and salinities become higher in runs DDP and GHD than in run CDD, and changes in run DDP are more than twice those in run GHD.

Results showed that the western boundary region is the most favorable place for double diffusion due to the differential advection of water masses by strong surface and deep western boundary currents. This is consistent with the known occurrence of salt fingers in the western tropical Atlantic (Schmitt et al. 1987) and their inferred role in water mass changes in the Caribbean Sea and Gulf of Mexico (Schmitz et al. 1993).

Sensitivity experiments show that the values of K^*, R_c, and n can affect the ratio of mixing due to double diffusion over the non-double-diffusive background mixing. When K^* or R_c are larger or n is smaller, mixing due to double diffusion intensifies. As a result, diapycnal diffusion of buoyancy is reduced, and the thermohaline circulation rate declines. The additional constraint of $T_{z,c}$ on T_z can affect the activity of double diffusion in the deep ocean and subpolar region, but it has no significant effect on the meridional overturning rate. Experiments with salt fingering only and diffusive layering only indicate that for a single-hemisphere basin under relaxation conditions for both temperature and salinity, salt fingering is dominant while diffusive layering activity is barely noticeable. However, diffusive layering could play a more important role under ''mixed'' type upper boundary conditions and in models that include a polar ocean. Higher vertical resolution appeared to improve the distribution of water masses, but the strength of the thermohaline circulation remained about the same. From the limited observational data available, the parameterization proposed in section 2 seems a reasonable first step to test the effects of double diffusion. Although we consider our parameterization to be rather conservative, its implementation led to significant changes in the circulation.

One of the more surprising results of this work was the finding that the introduction of double diffusion led to even more favorable conditions for its occurrence. Whereas in a one-dimensional simulation (Schmitt 1981) double diffusion operates to drive R_ρ away from one, its application in this general circulation model tended to generate even more areas with low density ratio. This is due to the double-diffusive redistribution of buoyancy, which produces pressure gradients that drive vertical shears that act on the isopycnal temperature and salinity gradients (Schmitt 1990). Such self-enhancing effects are well recognized in finescale thermohaline intrusions, but our results indicate that they operate on larger vertical scales as well.

These experiments with the ''standard'' relaxation boundary conditions are intended to presage an examination of double-diffusive effects in circulation models with mixed boundary conditions. It is our intention to evaluate the impact of double diffusion on the stability of GCMs with a flux, rather than restoring, boundary condition for the salinity. Such models typically display complex oscillatory behavior on a variety of timescales, and we anticipate a sensitivity of the circulation to the double-diffusive mixing in certain parameter regimes. However, even the present results, which reveal a reduction in the meridional overturning circulation, should motivate work toward an improved parameterization of the double-diffusive mixing processes.

Acknowledgments. Detailed comments from two reviewers helped us to improve the manuscript substantially. J.Z. and R.W.S. were supported by a grant from the Ocean Sciences Division of the National Science Foundation, OCE94-15589. R.X.H was supported by NSF through Grant OCE93-00706.

REFERENCES

Bryan, F., 1987: On the parameter sensitivity of primitive equation ocean general circulation model. *J. Phys. Oceanogr.,* **17,** 970–985.

Bryan, K., 1969: A numerical method for the study of the circulation of the world ocean. *J. Comput. Phys.,* **4,** 347–376.

Cummins, P. F., G. Holloway, and A. E. Gargett, 1990: Sensitivity of the GFDL ocean general circulation model to a parameterization of vertical diffusion. *J. Phys. Oceanogr.,* **20,** 817–830.

Danabasoglu, G., and J. C. McWilliams, 1995: Sensitivity of the global ocean circulation model to parameterizations of mesoscale tracer transports. *J. Climate,* **8,** 2967–2987.

Federov, K. N., 1988: Layer thicknesses and effective diffusivities in ''diffusive'' thermohaline convection in the ocean. *Small-Scale Turbulence and Mixing in the Ocean,* Vol. 46, J. Nihoul and B. Jamart, Eds., Elsevier, 471–480.

Gargett, A. E., and R. W. Schmitt, 1982: Observations of salt fingers in the central waters of the eastern North Pacific. *J. Geophys. Res.,* **87**(C10), 8017–8029.

——, and G. Holloway, 1992: Sensitivity of the GFDL ocean model to different diffusivities for heat and salt. *J. Phys. Oceanogr.,* **22,** 1158–1177.

——, and B. Ferron, 1996: The effects of differential vertical diffusion of T and S in a box model of thermohaline circulation. *J. Mar. Res.,* **54,** 827–866.

Garrett, C. J. R., and W. H. Munk, 1972: Oceanic mixing by breaking internal waves. *Deep-Sea Res.,* **19,** 823–832.

Gent, P. R., and J. C. McWilliams, 1990: Isopycnal mixing in ocean circulation models. *J. Phys. Oceanogr.,* **20,** 150–155.

——, J. Willebrand, T. J. McDougall, and J. C. McWilliams, 1995: Parameterizing eddy-induced tracer transports in ocean circulation models. *J. Phys. Oceanogr.,* **25,** 463–474.

Gregg, M. C., 1989: Scaling turbulent dissipation in the thermocline. *J. Geophys. Res.,* **94,** 9686–9698.

——, and T. B. Sanford, 1987: Shear and turbulence in the thermohaline staircases. *Deep-Sea Res.,* **34,** 1689–1696.
Hamilton, J. M., N. S. Oakey, and D. E. Kelley, 1993: Salt finger signatures in microstructure measurements. *J. Geophys. Res.,* **98**(C2), 2453–2460.
Hellerman, S., and M. Rosenstein, 1983: Normal monthly stress over the world ocean with error estimates. *J. Phys. Oceanogr.,* **13,** 1093–1104.
Hogg, N., P. Biscaye, W. Gardner, and W. J. Schmitz, 1982: On the transport and modification of Antarctic Bottom Water in the Vema Channel. *J. Mar. Res.,* **40** (Suppl.), 231–263.
Huang, R. X., 1993: Real freshwater flux as a natural boundary condition for the salinity balance and thermohaline circulation forced by evaporation and precipitation. *J. Phys. Oceanogr.,* **23,** 2428–2446.
——, 1995: *Advances in Theories of Wind-Driven and Thermohaline Circulation, a Lecture Series.* University of Hawaii at Manoa, SOEST, 213 pp.
——, and J. Yang, 1996: Deep-water upwelling in the frictional western boundary layer. *J. Phys. Oceanogr.,* **26,** 2243–2250.
Huppert, H. E., 1971: On the stability of a series of double-diffusive layers. *Deep-Sea Res.,* **18,** 1005–1021.
Ingham, M. C., 1966: The salinity extrema of the world ocean. Ph.D. thesis, Oregon State University, 63 pp. [Available from University Microfilms Inc., 300 North Zeeb Road, Ann Arbor, MI 48106-1346.]
Kelley, D. E., 1984: Effective diffusivities within oceanic thermohaline staircases. *J. Geophys. Res.,* **89,** 10 484–10 488.
——, 1990: Fluxes through diffusive staircases: A new formulation. *J. Geophys. Res.,* **95,** 3365–3371.
Kunze, E., 1990: The evolution of salt fingers in inertial wave shear. *J. Mar. Res.,* **48,** 471–504.
Ledwell, J. R., A. J. Watson, and C. S. Law, 1993: Evidence for slow mixing across the pycnocline from an open-ocean tracer-release experiment. *Nature,* **364,** 701–703.
Levitus, S., 1982: *Climatological Atlas of the World Ocean.* NOAA Prof. Paper No. 13. Govt. Printing Office, Washington, DC, 173 pp.
Lueck, R., 1987: Microstructure measurements in a thermohaline staircase. *Deep-Sea Res.,* **34,** 1677–1688.
Mack, S. A., 1985: Two-dimensional measurements of ocean microstructure: The role of double diffusion. *J. Phys. Oceanogr.,* **15,** 1581–1604.
——, 1989: Towed chain measurement of ocean microstructure. *J. Phys. Oceanogr.,* **19,** 1108–1129.
——, and H. C. Schoeberlein, 1993: Discriminating salt fingering from turbulence-induced microstructure: Analysis of towed temperature–conductivity chain data. *J. Phys. Oceanogr.,* **23,** 2073–2106.
Marmorino, G. O., W. K. Brown, and W. D. Morris, 1987: Two-dimensional temperature structure in the C-SALT thermohaline staircase. *Deep-Sea Res.,* **34,** 1667–1675.
Marotzke, J., 1997: Boundary mixing and the dynamics of three-dimensional thermohaline circulation. *J. Phys. Oceanogr.,* **27,** 1713–1728.
Martinson, D. G., 1990: Evolution of the Southern Ocean winter mixed layer and sea ice: open ocean deep water formation and ventilation. *J. Geophys. Res.,* **95,** 11 641–11 654.
McDougall, T. J., 1983: Greenland Sea Bottom Water formation: A balance between advection and double-diffusion. *Deep-Sea Res.,* **30,** 1109–1118.
——, and J. R. Taylor, 1984: Flux measurements across a finger interface at low values of the stability ratio. *J. Mar. Res.,* **42,** 1–14.
——, and J. A. Whitehead Jr., 1984: Estimates of the relative roles of diapycnal, isopycnal and double-diffusive mixing in Antarctic Bottom Water in the North Atlantic. *J. Geophys. Res.,* **89,** 10 479–10 483.
Muench, R. D., H. J. S. Fernando, and G. R. Stegen, 1990: Temperature and salinity staircases in the northwestern Weddell Sea. *J. Phys. Oceanogr.,* **20,** 295–306.
Munk, W. H., 1966: Abyssal recipes. *Deep-Sea Res.,* **13,** 707–730.
Neal, V. T., S. Neshyba, and W. Denner, 1969: Thermal stratification in the Arctic Ocean. *Science,* **166,** 373–374.
Neshyba, S., V. T. Neal, and W. W. Denner, 1971: Temperature and conductivity measurements under Ice Island T-3. *J. Geophys. Res.,* **76,** 8107–8120.
Pacanowski, R. C., 1995: MOM2 documentation, user's guide and reference manual. Tech. Rep. 3, GFDL Ocean Group Technical Report 232 pp. [Available from online at http://www.gfdl.gov/~kd/momwebpages/momwww.html.]
Padman, L., and T. M. Dillon, 1987: Vertical fluxes through the Beaufort Sea thermohaline staircase. *J. Geophys. Res.,* **92,** 10 799–10 806.
——, and ——, 1988: On the horizontal extent of the Canada Basin thermohaline steps. *J. Phys. Oceanogr.,* **18,** 1458–1462.
Polzin, K., 1996: Statistics of the Richardson Number: Mixing models and finestructure. *J. Phys. Oceanogr.,* **26,** 1409–1425.
——, J. M. Toole, and R. W. Schmitt, 1995: Finescale parameterizations of turbulent dissipation. *J. Phys. Oceanogr.,* **25,** 306–328.
——, ——, J. R. Ledwell, and R. W. Schmitt, 1997: Spatial variability of turbulent mixing in the abyssal ocean. *Science,* **276,** 93–96.
Redi, M. H., 1982: Oceanic isopycnal mixing by coordinate rotation. *J. Phys. Oceanogr.,* **12,** 1154–1158.
Robertson, R., L. Padman, and M. D. Levine, 1995: Finestructure, microstructure, and vertical mixing processes in the upper ocean in the western Weddell Sea. *J. Geophys. Res.,* **100,** 18 517–18 535.
Ruddick, B., 1983: A practical indicator of the stability of the water column to double-diffusive activity. *Deep-Sea Res.,* **30,** 1105–1107.
——, 1992: Intrusive mixing in a Mediterranean salt lens: Intrusion slopes and dynamical mechanisms. *J. Phys. Oceanogr.,* **22,** 1274–1285.
——, and J. S. Turner, 1979: The vertical length scale of double-diffusive intrusions. *Deep-Sea Res.,* **26A,** 23–40.
——, and L. Zhang, 1989: The mythical thermohaline oscillator? *J. Mar. Res.,* **47,** 717–746.
Schmitt, R. W., 1979: The growth rate of super-critical salt fingers. *Deep-Sea Res.,* **26A,** 23–40.
——, 1981: Form of temperature–salinity relationship in the central water: Evidence for double-diffusive mixing. *J. Phys. Oceanogr.,* **11,** 1015–1026.
——, 1988: Mixing in a thermohaline staircase. *Small-Scale Turbulence and Mixing in the Ocean,* Vol. 46, *Elsevier Oceanogr. Ser.,* J. Nihoul and B. Jamart, Eds., Elsevier, 435–452.
——, 1990: On the density ratio balance in the Central Water. *J. Phys. Oceanogr.,* **20,** 900–906.
——, 1994: Double diffusion in oceanography. *Annu. Rev. Fluid Mech.,* **26,** 255–85.
——, H. Perkins, J. D. Boyd, and M. C. Stalcup, 1987: C-SALT: An investigation of the thermohaline staircase in the western tropical North Atlantic. *Deep-Sea Res.,* **34,** 1697–1704.
Schmitz, W. J., J. R. Luyten, and R. W. Schmitt, 1993: On the Florida current T/S envelope. *Bull. Mar. Sci.,* **53,** 1048–1065.
Shen, C., and R. W. Schmitt, 1995: The wavenumber spectrum of salt fingers. *Double-Diffusive Convection,* A. Brandt and H. Fernando, Eds., Vol. 94, Amer. Geophys. Union, 305–312.
Shirtcliffe, T. G. L., 1967: Thermosolutal convection: Observation of an overstable mode. *Nature,* **213,** 489–490.
Stern, M. E., 1960: The ''salt fountain'' and thermohaline convection. *Tellus,* **12,** 172–175.
——, 1975: *Ocean Circulation Physics.* Academic Press, 246 pp.
Stommel, H., and A. B. Arons, 1960: On the abyssal circulation of the world ocean. Part II: An idealized model of the circulation pattern and amplitude in oceanic basins. *Deep-Sea Res.,* **6,** 339–343.
Taylor, J., 1991: Laboratory experiments on the formation of salt

fingers after the decay of turbulence. *J. Geophys. Res.,* **96**(C7), 12 497–12 510.
Toole, J. M., K. L. Polzin, and R. W. Schmitt, 1994: Estimates of diapycnal mixing in the abyssal ocean. *Science,* **264,** 1120–1123.
Turner, J. S., 1973: *Buoyancy Effects in Fluids.* Cambridge University Press, 367 pp.
——, 1978: Double-diffusive intrusions into a density gradient. *J. Geophys. Res.,* **83,** 2887–2901.
Weaver, A. J., and E. S. Sarachik, 1990: On the importance of vertical resolution in certain ocean general circulation models. *J. Phys. Oceanogr.,* **20,** 600–609.
——, and T. M. C. Hughes, 1992: Stability and variability of the thermohaline circulation and its link to climate. *Trends Phys. Oceanogr.,* **1,** 15–70.
Yin, F. L., and I. Y. Fung, 1991: Net diffusivity in ocean general circulation models with nonuniform grids. *J. Geophys. Res.,* **96,** 10 773–10 776.
Zhang, J., R. W. Schmitt, and R. X. Huang, 1997: The relative influence of diapycnal mixing and hydrologic forcing on the stability of the thermohaline circulation. *J. Phys. Oceanogr.,* submitted.